Willumeit, R.; Feyerabend, F.; Huber, N.:

Magnesium degradation as determined by artificial neural networks

In: Acta Biomaterialia (2013) Elsevier

DOI: 10.1016/j.actbio.2013.02.042

Magnesium degradation as seen by artificial neural networks (ANN)

Regine Willumeit, Frank Feyerabend, Norbert Huber

Institute of Materials Research, Helmholtz-Zentrum Geesthacht, Max-Planck-Str. 1, 21502 Geesthacht, Germany

Email: regine.willumeit@hzg.de, frank.feyerabend@hzg.de, norbert.huber@hzg.de

Corresponding Author:

Prof. Dr. Regine Willumeit

Institute of Materials Research

Helmholtz-Zentrum Geesthacht

Max-Planck-Str. 1

21502 Geesthacht

Germany

Tel.: +49 170 4316430

Fax: +49 04152 872666

Email: regine.willumeit@hzg.de

1. Introduction

Magnesium, which is a degradable metal, has considerable potential for biomedical applications. The physical and mechanical properties of magnesium are comparable to that of bone [1], and since the last century [2], magnesium has been known as a suitable implant material for enhanced healing and mineralisation [3-4] if corrosion is controlled. However, the mechanism for the degradation of magnesium has not yet been clarified, despite the availability of *in vivo* data [5-7] and clinical trials [8-10].

The comparison of *in vitro* and *in vivo* data is very difficult because the majority of the parameters that can influence the degradation of magnesium cannot be easily measured *in vivo* [11]. Therefore, finding appropriate *in vitro* tests, despite available normative and standardisation procedures (e.g., ISO 10993 [12] or ASTM-G31-72 [13]), is a significant obstacle [14-15]. For example, in animal trials, it has been observed that the corrosion rate was slowed by several orders of magnitude compared to *in vitro* tests using standard laboratory corrosion solutions [16], which indicates that the use of relatively simple corrosion solutions is not sufficient to describe the complex chemical reactions that occur in the body [17-18]. However, even if realistic physiological conditions are avoided, the description of events during the corrosion process is already difficult when substances in addition to water and NaCl are present. Several explanations have been provided for the corrosion behaviour in Simulated Body Fluid (SBF) or other standard electrolyte solutions (Hank's balanced salt solution (HBSS), phosphate buffered saline (PBS), etc.) that lack proteins; the high amount of chloride in the corrosion media leads to high corrosion rates [19-21]. When using more complex media, such as cell growth media (e.g., Dulbeco's Modified Eagle Medium (DMEM) or Eagle's Minimum Essential Medium (EMEM)), the additional inorganic and organic compounds significantly alter

the corrosion behaviour [22]. Changing to solutions that in addition contain proteins also provides different results, which usually produces a decrease in the corrosion rate (e.g., [22-25]) and alters compositions of the corrosion layer [26]. If measurements are performed under cell culture conditions, the influence of O_2 and CO_2 is also observed, and the ratio of the resulting corrosion products is shifted compared to those under atmospheric conditions [27-29].

In general, reports on the *in vitro* and *in vivo* degradation of magnesium are more descriptive rather than offering a realistic chemical explanation of the processes [1, 30-32]. One further drawback is that the corrosion products are generally not actually analysed because determination of the corrosion rates is performed after removing the corrosion layers. Furthermore, qualitative *in vivo* studies are lacking, which makes the comparison of highly complex *in vitro* systems with processes occurring *in vivo* nearly impossible [30]. Because we are far from a full understanding of the reactions, in this paper, we attempt to find correlations between the parameters that can be observed during the corrosion process *in vitro* using an Artificial Neural Network (ANN). We would like to answer the questions of what experimental conditions have a significant influence on the corrosion rate and whether synergistic or antagonistic effects can be identified. To illustrate the problem, Fig. 1 displays the measured Mg corrosion rate in DMEM. A simple summation of the values at 20°C with and without CO_2 and at 37°C without CO_2 does not automatically lead to a prediction of the corrosion rate at 37°C in the presence CO_2. Adding proteins decreases the corrosion rate in all cases – but is there a correlation between temperature, protein availability and CO_2 content?

ANNs mimic two features of the brain: the complexity and one principal step in signal transmission. In the brain, we have several hundreds of billion neurons, and each neuron is connected to thousands of neighbouring neurons. This feature is

represented by the number of nodes and “hidden layers” in the ANN. To transmit a signal from one neuron to the next, the receiving neuron sums up the arriving chemical or electrical information until a certain threshold value is reached. After this threshold is reached, the neuron fires its signals to its neighbours. This step is also essential in the ANN, where an adjustable threshold in the neurons regulates when the input is transmitted to the following neurons.

ANNs are widely used in materials science, but they are also used in biological or medical studies (e.g., [33-36]). Only a few works can be found on the prediction of degradation behaviour of medical implants using an ANN [37-38]. Here, we apply this method to analyse the correlation of nine parameters with respect to the measured corrosion rate of extruded pure Mg. We used different levels of O_2 (5 and 21%), CO_2 (0, 2.5 and 5%), proteins (FBS, 0, 10 and 20% by volume), and glucose (0 – 4.5 g/L), changes in temperature (20 and 37°C) and the composition of different corrosion media (water, HBSS and DMEM) (69 parameter sets) as the input parameters.

2. Materials & Methods

2.1 Material

Magnesium (99.94 %, Magnesium Elektron, UK) was melted in a mild steel crucible under a protective atmosphere (Ar + 2 % SF_6). Ingots were produced by permanent mould direct chill casting [39]. The ingot was extruded to a 12 mm rod. Specimens (d = 10 mm, h = 1.5 mm) were machined from the rod and sterilised by ultrasonic treatment for 20 min in 70% ethanol.

2.2 Determination of corrosion rate

The corrosion rate was determined based on the weight loss after immersion for 72 h in distilled water, water with 3 g/L NaCl (Merck, Darmstadt, Germany), water with 3

g/L NaCl and 4.5 g/L glucose (Sigma-Aldrich Chemie, Taufkirchen, Germany), Hank's balanced salt solution (HBSS, Life Technologies, Darmstadt, Germany) or Dulbecco's modified eagle medium (DMEM, Life Technologies). 10 and 20% FBS (PAA Laboratories, Linz, Austria) were added to all of the solutions. Incubation was performed under atmospheric (20 and 37°C) and cell culture conditions with variations in the O_2 (5 and 21%) and CO_2 (2.5 and 5%) concentrations. The samples were weighed before immersion. After immersion, the corrosion products were removed by immersion in chromic acid (180 g/L; VWR International, Darmstadt, Germany) for 20 min at room temperature. The average corrosion rate was calculated in units of mm/year with the equation

$$CR = \frac{8.76 \times 10^4 \, \Delta g}{A \cdot t \cdot \rho} \tag{1}$$

where Δg is the weight change (in g), A is the surface area (in cm^2), t is the immersion time (in h), and ρ is the density of the alloy (in g cm^{-3}).

2.3 Neural Networks

ANNs represent a qualified tool for solving complex problems. ANNs are flexible functions that can be trained to represent any unique relationship given by a number of examples. The training data (patterns) consist of pairs of function values (outputs, y_l) and function arguments (inputs, x_i). The best definition of the inputs is part of the ANN development and will be described in detail in sections 3.1 and 3.2. As the output, we have a single output neuron, which predicts the corrosion rate.

In this work, feed forward neural networks are used, which are organised as a hierarchical neural network with an input layer, one hidden layer and an output layer [40]. The smooth sigmoidal function is chosen as the activation function. Training is performed by minimising the value of the error function

$$E = \sum_{p} (d_p - y_p)^2 + 10^{-\kappa} \sum {w_{ij}}^2 \,. \qquad (2)$$

The first term of Eq. (2) represents the error sum of the single output y_p and the desired value of the corrosion rate d_p for a given pattern p (measured corrosion rate for a set of parameters). The second term of Eq. (2) is the normalised synaptic weight vector w_{ij}. The synaptic weights can be interpreted as the parameters of a flexible nonlinear vector function (the ANN), which need to be calibrated during the training process. If the synaptic weights are allowed to take large values, the ANN tends to classify. To avoid such classification, which is also called over-learning, the value of the training parameter κ is typically chosen between 5 and 6 to obtain a smooth approximation of the training patterns.

In minimising the error E, both the output error and the values of the synaptic weights will be adjusted to be as small as possible, thus improving the generalisation of the network. The training algorithm refers to the RPROP algorithm [41], which allows batch learning (simultaneous optimisation of all patterns) and is very quick and stable. In this algorithm, one optimisation increment that improves the synaptic weights for all patterns corresponds to one epoch. The applied neural network simulation and training software has been used in previous works (e.g., see [42]). After training, the saved ANN code can be called by a Python code, which allows for mapping the corrosion rate as function of the input parameters x_i. In this manner, the stored relationship between the inputs and output can be smoothly analysed by continuous variations of x_i, independent of the original location of the individual training patterns.

3. Results

3.1 Development of data base

The data base is the key for providing the relevant information for ANN training. For a successful approximation of the multi-parameter space, it is important to efficiently distribute the experiments in the training space. The typical experimental approaches of changing only one parameter at a time lead to the multiple allocation of certain values for a given input. Generating such a pattern represents a waste of potential information on the effect of all the other inputs. Even more problematic is the trend of ANNs to classification rather than generalisation if a multi-parameter space contains only a few patterns.

Fig. 2 presents the experimental data, where the dependence of the corrosion rate on the CO_2 and buffer (represented by the concentration of NaCl) was measured. Additional variations in the O_2 concentration, protein concentration and temperature lead to the vertical distribution of the data points above a grid point defined by CO_2 and NaCl.

In the first series of experiments (Data Set #1, spheres, 36 measurements), the data points show a clear trend of increasing corrosion rate with increasing CO_2 concentration. However, this data set does not reveal any information between 0 and 5 % CO_2, and thus, the ANN could freely choose its shape between these two values during training. The large gap, which exists for the NaCl concentrations between 0 and 6400 mg/L, could induce a similar problem. Consequently, poor generalisation within this undefined training space would result.

To also provide information in this area, additional grid points were defined and a second set of experiments was conducted (Data Set #2, stars). Viewing both data sets together (69 measurements total), the previously observed qualitative increase

of the corrosion rate with increasing CO_2 concentration is still visible, but an easy understanding of the underlying dependencies is now obviously difficult.

With the aid of the ANN, we will follow a two-step strategy, where the importance of individual parameters will be initially identified followed by ANN analysis of the data base with a selection of important input parameters. Table 1 presents the ranges of the measured corrosion rates and the parameters that define the training space.

3.2 Identification of important parameters

A first impression of the information content of a certain parameter with respect to the corrosion rate can be obtained from the training of an ANN with a 1-3-1 architecture, i.e., one input neuron, three hidden neurons and one output neuron. We provide one input parameter and train the network to predict the corrosion rate based only on this single piece of information. As an extension to a conventional correlation analysis, the ANN is given some flexibility to mimic a nonlinear one-to-one relationship through the three hidden neurons. All of the ANNs are trained by 1000 epochs. As a quality measure, we use the mean square error $\sum(d_p - y_p)^2 / P$, where $p \in \{1,..,P\}$ is the pattern number used for the training of the ANN. The results for all of the possible input parameters, which are sorted by increasing mean square error, are presented in Fig. 3. The lower the error, the better the ANN can predict the corrosion rate from the given input parameter. From the ranking of the parameters in Fig. 3, we can see that the two most important parameters are CO_2 and NaCl, followed by the other buffer contents.

The three buffer contents $NaHCO_3$, $MgSO_4$ and $CaCl_2$ present the same error. This result is due to a direct correlation of these three buffer contents as a consequence of preparing the different buffer systems. Therefore, $CaCl_2$ and $MgSO_4$ carry no additional independent information; they are linearly dependent on $NaHCO_3$. For the

subsequent analysis of the effect of $NaHCO_3$ with respect to the other independent parameters, it is necessary to eliminate $MgSO_4$ and $CaCl_2$ as possible inputs.

In a more refined step, a second type of ANN with a 6-3-1 architecture is trained, which is based on the following selected inputs: CO_2, NaCl, $NaHCO_3$, O_2, T, glucose, and protein. By subsequently removing only one of these seven inputs, the relevance of the related input information can be determined. The larger the increase in the error, the more important the missing information is. The ANN trained with all seven inputs serves as a reference (7-3-1 architecture). The comparison of the results presented in Fig. 4 with those of Fig. 3 leads to the following conclusions: (a) there is agreement that CO_2 and NaCl are parameters of high importance; (b) temperature and $NaHCO_3$ are of medium importance; and (c) glucose is of lowest importance.

In contrast to Fig. 3, Fig. 4 reveals that O_2 has also an important effect, which appears to be even larger than that of NaCl. Furthermore, the role of the protein is comparable to that of temperature and $NaHCO_3$. Because of these observations, only glucose will be eliminated from further investigations. The effects of temperature, protein and $NaHCO_3$ should be further investigated in more detail.

3.3 Analysis of ANN prediction

In this subsection, five ANNs are trained with identical input definitions, network structure (6-3-1) and training duration (10000 epochs). These ANNs differ only in the initial random setting of the synaptic weights. The six inputs are defined by the following parameters: CO_2, O_2, NaCl, temperature, protein and $NaHCO_3$. After training, the evaluation of the five ANN outputs allows an expected value and a standard deviation to be derived for a given set of inputs. In this way, we gain additional insight into the reliability of the prediction – or uncertainty of the ANN training – depending on the position in the parameter space. This statistical approach

could be further refined in the future through the use of Bayesian Neural Networks, where distributions of ANNs can be generated according to their probability with respect to the presented set of training patterns [43].

After training, the performance of the averaged ANN response is checked with respect to the re-prediction of the original training data (combined Data Set #1 and #2). In Fig. 5a, the predicted (averaged) ANN output is plotted versus the desired value for all of the training patterns. The error bar indicates the standard deviation derived from the five ANN responses for the individual training patterns. Fig. 5b presents the absolute values of all errors $|y_p - d_p|$, which are sorted by increasing error value and plotted versus the normalised pattern number p/P. It can be observed that the error in the predicted corrosion rate is less than 0.55 mm/year for 90% of the training patterns. This error band, which is denoted as a 90% confidence interval, is included in Fig. 5a (dashed lines correspond to the desired value of the corrosion rate, ±0.55 mm/year). Fig. 5a also reveals that only a few predictions exhibit a significant standard deviation that is comparable to the 90% confidence interval.

A first evaluation of the ANN response for the reference case, which is defined as O_2 = 21%, T = 20°C and the absence of protein and $NaHCO_3$, is shown in Fig. 6. Fig. 6a presents the expected value, which is averaged from the five ANNs. In the absence of CO_2, a monotonic increase in the corrosion rate can be observed with increasing NaCl; the ANNs predict a maximum at a CO_2 concentration of 5%. This behaviour is in agreement with the data shown in Fig. 2, where the additional values of Data Set #2 (stars) show this clear maximum.

The standard deviation, which is plotted in Fig. 6b, is in agreement with the provided data base. The density of the data is high, and the standard deviation of the ANN prediction is low along the boundaries with the lowest and highest NaCl

concentrations. In the centre region, we have a lower density of patterns leading to a maximum standard deviation of approximately 1 mm/year for the ANN prediction.

From the discussion with regard to Figs. 3 and 4, it is still unclear in which combination and in which region certain parameters become important. In the following, we use the ANN to investigate the effects of O_2, temperature, protein, and $NaHCO_3$. For a better comparison, the effect of each of these parameters is studied individually.

The results are presented in Fig. 7 as the change in the corrosion rate with respect to the reference case, which was shown in Fig. 6a. In this plot, a noticeable effect for O_2 and $NaHCO_3$ can be observed. For medium and high CO_2 concentrations, a reduction in the O_2 concentration from 21 to 5% increases the corrosion rate by more than 1 mm/year. Adding $NaHCO_3$ can decrease the corrosion rate by approximately 1.5 mm/year. In contrast to O_2, the effect here is larger for low CO_2 concentrations. Protein and temperature only have an intermediate but opposite effect for high CO_2 concentrations, whereas for a low CO_2 concentration, the effect of both is negligible. At high CO_2 concentrations, an increase in protein slightly decreases the corrosion rate while an increase in temperature slightly increases the corrosion rate by approximately 0.5 mm/year.

4. Discussion

The ANN analysis in section 3.3 revealed that the concentrations of CO_2 and certain buffer contents, such as NaCl, are very important for the corrosion rate (up to 3 mm/year). Following are O_2 and $NaHCO_3$ with an effect of approximately 1.5 mm/year, while proteins and temperature have only an intermediate effect of approximately 0.5 mm/year, depending on the CO_2 concentration. The lowest impact results from glucose; its omission did not impair the prediction of the ANN. The

insensitivity to protein and temperature changes at lower CO_2 concentrations suggests a robust ANN prediction. However, the standard deviation of the ANN prediction reached 1 mm/year in the centre of the training regime where only a few training patterns are available. Therefore, the results must still be viewed with caution, and further work should be conducted to add more training patterns in regions with higher ANN standard deviations.

The ANN analysis provides us with information about the relevance of different parameters that influence the corrosion rate and might provide an indication of how *in vitro* assessments of new biodegradable alloys should be performed. However, in the context of medical applications, papers can currently be found where magnesium corrosion is measured at room temperature and in more or less physiological solutions [44-45]. The increase of temperature to 37°C, which can easily be achieved, is still not a standard procedure. However, in recent years, it has become more evident that considering additional parameters is beneficial for the correlation of Mg corrosion *in vitro* and *in vivo*. In addition to the increase of the temperature to a meaningful range, f.e. SBF with HEPES or TRIS are used to at least partially the mimic buffering capacity of blood [46-52]. However, despite an ongoing discussion about the appropriateness of using SBF [53], it is often disregarded that the buffering capacity of most solutions is dependent on the supply of gaseous CO_2, which is also the mechanism of blood buffering capacity [54]. The use of cell culture medium is not obvious, but it has become more popular [17, 27, 55-57]. However, even in high quality publications, a critical discussion on the differences in the corrosion rate when comparing measurements under standard conditions with cell culture conditions or *in vivo* studies is not considered [58]. To come closer to *in vivo* – without knowing what that entails exactly – the influence of proteins [26, 59] or the implementation of flow [60] is considered. While proteins should reduce the corrosion rate by mere adhesion

and the direct electrostatic interaction of Mg^{2+} to bind the protein to the surface [23, 59, 61] or by changing the composition of the corrosion layer [26], flow will increase the corrosion rate due to a pH value that is maintained in the neutral range.

In addition to this phenomenological description of the influence of external parameters on the degradation behaviour, the chemical reactions that are discussed in the context of Mg degradation are usually oversimplified [62] and do not consider that solubility is dependent on pH, the common-ion effect, temperature, the ionic strength of the solution and pressure [63].

To summarise: the information that we have on the corrosion of Mg under physiological conditions is very limited, and due to the highly complex system, a thorough chemical description of the involved processes is experimentally difficult and very time consuming to obtain. Here, the ANN analysis that is ideally suited to investigate non-linear relationships with multiple inputs can be used to identify the primary influences on the corrosion of Mg.

From the nine input parameters, the ANN analysis clearly revealed an important influence of the presence of CO_2 on the corrosion rate, which indicates that cell culture conditions should be implemented during corrosion measurements. The physiological relevance is obvious: In ambient air, 0.034% CO_2 is present, whereas in blood and bone, CO_2 values are found that are comparable to the applied amount of 5% CO_2 under the cell culture conditions (Tab. 2).

The presence of CO_2 might trigger several reactions that influence the corrosion process. When dissolved in water, CO_2 leads to the formation of H_2CO_3, which can then dissociate to H_3O^+ and HCO_3^-. The latter, hydrogen carbonate, plays an important role in the buffering system of the blood and the corrosion solution by maintaining a neutral pH. In parallel, HCO_3^- can react with H_2O to form CO_3^{2-} and

H_3O^+, which causes the pH to become basic, which also has an effect on the corrosion rate of Mg.

Oxygen, which was the second gaseous compound in our system, does not have such a strong influence on the corrosion rate of Mg. This result might be related to the fact that O_2 does not change the pH and that it most likely does not directly interact with Mg. To mimic *in vivo* conditions, a reduction of O_2 is recommended because under *in vivo* conditions, the content of oxygen in many tissues is approximately 1-7%, which is less than that of ambient air (21%)[64-66] (Tab. 2). The present study indicates that O_2 is not important when 5% CO_2 is present. At low CO_2 concentrations, however, a reduction of O_2 can increase the corrosion rate by 1 mm/year.

In the presence of 5% CO_2, the inclusion of an elevated temperature causes an intermediate effect on the corrosion rate due to the increase of the reaction constants. Therefore, this parameter should also be included in *in vitro* experiments.

The second parameter that has an intermediate effect on the corrosion rate is the presence of proteins. Here, it is striking that proteins are not found to be one of the prominent factors that reduces the corrosion rate because they are expected to be the most likely candidate to bridge the gap between *in vitro* and *in vivo*. Many proteins are able to bind Mg^{2+}-ions [67] and for Human Serum Albumin (HSA), which is the human analogue to Bovine (B)SH and the primary component of FBS, it has been reported that between 2 – 10 ions can attach to the protein [68-73]. This fact may explain, in general, the deceleration of the corrosion processes that were also observed *in vitro* (see Fig. 1). However, the ANN does not reveal a very strong impact on the parameter under investigation, the corrosion rate. This result could lead in another direction, namely that the presence of proteins alters the composition of the corrosion layer by introducing additional interactions with the primary corrosion

products [26] but has no direct influence on the velocity of the corrosion process itself. In parallel, the interaction of proteins with the contents of the chosen solutions (e.g., calcium depletion) was observed in earlier studies ([29]).

Another possibility to explain why the ANN does not reveal an important influence of proteins on the corrosion rate might be that we have integrated the measurements over 72 hours. Time resolved studies under cell culture conditions have revealed that the release of Mg-ions into the corrosion medium is significantly increased in the presence of FBS within the first 24 h due to pH stabilisation [27], whereas it slows down over time.

A very complicated issue is the influence of the different components of the corrosion solution. Obviously, we can observe a non-linear behaviour for NaCl that depends on a currently unidentified cross reaction. The ANN analysis identified $NaHCO_3$ in presence of 5% CO_2 as possible counterpart (see Fig. 7). A possible cross reaction could be $NaHCO_3 \rightarrow Na^+ + HCO_3^-$ [74], which is involved in the buffering system under the influence of CO_2 and interferes with the equilibrium of NaCl dissociation and consequently the effects of Cl^- on Mg corrosion.

Glucose has been identified as the least influencing parameter. Glucose does not necessarily interact with any of the available partners. In water, the open-chain form of the molecule is found in equilibrium with its cyclic isomers, but no reports have been found concerning whether tautomerisation ions can bind and prevent ring formation.

In summary, ANN analysis provides the first evidence on what parameters are important for reliable *in vitro* test conditions (namely CO_2 and NaCl). In addition, we can separate the parameters into parameters of first and second order relevance. “First Order Relevance” consists of parameters such as CO_2, the presence of NaCl and $NaHCO_3$ and temperature that directly influence the corrosion rate. “Second

Order Relevance" consists of parameters such as O_2 and proteins that influence the corrosion layer and the final corrosion products. These parameters might also influence the cell reaction *in vivo*.

The consideration of flow, which has not been implemented in this study but is noteworthy in general, is a very important aspect not only for cardiovascular applications because the blood flow in tissue varies dramatically; in the cardiovascular system, velocities of more than 6000 mL/min have been measured [75-76], whereas in bone, flow rates between 0.08 and 0.125 mL/g/min have been measured [64, 77]. This aspect additionally raises complexity but is also an indication that *in vitro* setups should be established in a tissue-specific way [78].

5. Conclusions

ANN analysis represents a useful tool to approximate and analyse the complex non-linear reactions that occur during the corrosion of Mg under physiological conditions. Combining ANN analysis with the planning of further experiments allows regions to be identified where additional experiments should be placed either to gain a more robust prediction or to add missing information that was identified by ANN. The experimental effort can be reduced by omitting parameters of negligible influence.

With respect to the long-term goal of simulating *in vivo* testing with *in vitro* experiments, the importance of controlling the CO_2 concentration at 5% has been demonstrated. While the effect of O_2 appears to be minor in the presence of CO_2, NaCl and $NaHCO_3$ appear to significantly influence the corrosion rate through a yet unidentified cross reaction, which may also depend on temperature. Therefore, parameters of intermediate importance, such as temperature and protein, should be considered in future work with the goal of predicting the corrosion rate with accuracies greater than 1 mm/year.

6. Acknowledgements

We wish to thank Daniela Lange who skilfully performed the corrosion measurements and Sören Müller, Strangpreßzentrum, Berlin, for the extrusion of the Mg. The results of Fig. 1 were prepared by Tie Di (Helmholtz-Zentrum Geesthacht) and Wolf-Dieter Müller (Charité Berlin), and we gratefully acknowledge their experimental support.

References

[1] Staiger MP, Pietak AM, Huadmai J, Dias G. Magnesium and its alloys as orthopedic biomaterials: A review. Biomaterials 2006;27:1728-34.

[2] McBride E. Absorbable metal in bone surgery: A further report on the use of magnesium alloys. JAMA: The Journal of the American Medical Association 1938;111:2464-7.

[3] Maier O. Über die Verwendbarkeit von Leichtmetallen in der Chirurgie (metallisches Magnesium als Reizmittel zur Knochenneubildung). Deutsche Zeitschrift für Chirurgie 1940;253:552-6.

[4] Znamenskii MS. Metallic osteosynthesis by means of an apparatus made of resorbing metal. Khirurgiia 1945;12:60-3.

[5] Witte F, Kaese V, Haferkamp H, Switzer E, Meyer-Lindenberg A, Wirth CJ, et al. In vivo corrosion of four magnesium alloys and the associated bone response. Biomaterials 2005;26:3557-63.

[6] Castellani C, Lindtner RA, Hausbrandt P, Tschegg E, Stanzl-Tschegg SE, Zanoni G, et al. Bone–implant interface strength and osseointegration: Biodegradable magnesium alloy versus standard titanium control. Acta Biomaterialia 2011;7:432-40.

[7] Aghion E, Levy G, Ovadia S. In vivo behavior of biodegradable Mg–Nd–Y–Zr–Ca alloy. Journal of Materials Science: Materials in Medicine 2012;23:805-12.

[8] Di Mario C, Griffiths H, Goktekin O, Peeters N, Verbist J, Bosiers M, et al. Drug-eluting bioabsorbable magnesium stent. J Interv Cardiol 2004;17:391-5.

[9] Eggebrecht H, Rodermann J, Hunold P, Schmermund A, Bose D, Haude M, et al. Images in cardiovascular medicine. Novel magnetic resonance-compatible coronary stent: the absorbable magnesium-alloy stent. Circulation 2005;112:e303-4.

[10] Erbel R, Di Mario C, Bartunek J, Bonnier J, de Bruyne B, Eberli FR, et al. Temporary scaffolding of coronary arteries with bioabsorbable magnesium stents: a prospective, non-randomised multicentre trial. Lancet 2007;369:1869-75.

[11] Schumacher S, Stahl J, Bäumer W, Seitz JM, Bach F-W, Petersen LJ, et al. Ex vivo examination of the biocompatibility of biodegradable magnesium via microdialysis in the isolated perfused bovine udder model. Int J Artif Organs 2011;34:34-43.

[12] ISO. ISO 10993 - Biologische Beurteilung von Medizinprodukten. International Organisation for Standardization; 1999.

[13] ASTM. G31 - 72(2004) Standard Practice for Laboratory Immersion Corrosion Testing of Metals. ASTM International, West Conshohocken, PA; 2004. p. 8.

[14] Kirkland NT, Birbilis N, Staiger MP. Assessing the corrosion of biodegradable magnesium implants: A critical review of current methodologies and their limitations. Acta Biomaterialia 2012;8:925-36.

[15] Walker J, Shadanbaz S, Kirkland NT, Stace E, Woodfield T, Staiger MP, et al. Magnesium alloys: Predicting in vivo corrosion with in vitro immersion testing. Journal of Biomedical Materials Research Part B: Applied Biomaterials 2012;100B:1134-41.

[16] Witte F, Fischer J, Nellesen J, Crostack HA, Kaese V, Pisch A, et al. In vitro and in vivo corrosion measurements of magnesium alloys. Biomaterials 2006;27:1013-8.

[17] Liu H. The effects of surface and biomolecules on magnesium degradation and mesenchymal stem cell adhesion. Journal of Biomedical Materials Research Part A 2011;99A:249-60.

[18] Waizy H, Seitz J-M, Reifenrath J, Weizbauer A, Bach F-W, Meyer-Lindenberg A, et al. Biodegradable magnesium implants for orthopedic applications. J Mater Sci 2012:1-12.

[19] Mueller W-D, Fernández Lorenzo de Mele M, Nascimento ML, Zeddies M. Degradation of magnesium and its alloys: Dependence on the composition of the synthetic biological media. Journal of Biomedical Materials Research Part A 2009;90A:487-95.

[20] Song G. Control of biodegradation of biocompatable magnesium alloys. Corrosion Science 2007;49:1696-701.

[21] Zeng R-c, Zhang J, Huang W-j, Dietzel W, Kainer KU, Blawert C, et al. Review of studies on corrosion of magnesium alloys. Transactions of Nonferrous Metals Society of China 2006;16, Supplement 2:s763-s71.

[22] Yamamoto A, Hiromoto S. Effect of inorganic salts, amino acids and proteins on the degradation of pure magnesium in vitro. Materials Science and Engineering C 2009;29:1559–68.

[23] Liu C, Xin Y, Tian X, Chu PK. Degradation susceptibility of surgical magnesium alloy in artificial biological fluid containing albumin. J Mater Res 2007;22:1806-14.

[24] Rettig R, Virtanen S. Time-dependent electrochemical characterization of the corrosion of a magnesium rare-earth alloy in simulated body fluids. J Biomed Mater Res A 2008;85:167-75.

[25] Wang Y, Lim CS, Lim CV, Yong MS, Teo EK, Moh LN. In vitro degradation behavior of M1A magnesium alloy in protein-containing simulated body fluid. Materials Science and Engineering: C 2011;31:579-87.

[26] Willumeit R, Fischer J, Feyerabend F, Hort N, Bismayer U, Heidrich S, et al. Chemical surface alteration of biodegradable magnesium exposed to corrosion media. Acta Biomaterialia 2011;7:2704-15.

[27] Feyerabend F, Drücker H, Laipple D, Vogt C, Stekker M, Hort N, et al. Ion release from magnesium materials in physiological solutions under different oxygen tensions. Journal of Materials Science: Materials in Medicine 2012;23:9-24.

[28] Johnson I, Perchy D, Liu H. In vitro evaluation of the surface effects on magnesium-yttrium alloy degradation and mesenchymal stem cell adhesion. Journal of Biomedical Materials Research Part A 2012;100A:477-85.

[29] Yang L, Hort N, Willumeit R, Feyerabend F. Effects of corrosion environment and proteins on magnesium corrosion. Corrosion Engineering, Science and Technology 2012;47:335-9.

[30] Witte F, Hort N, Vogt C, Cohen S, Kainer KU, Willumeit R, et al. Degradable biomaterials based on magnesium corrosion. Current Opinion in Solid State and Materials Science 2008;12:63-72.

[31] Zhang S, Li J, Song Y, Zhao C, Zhang X, Xie C, et al. In vitro degradation, hemolysis and MC3T3-E1 cell adhesion of biodegradable Mg–Zn alloy. Materials Science and Engineering: C 2009;29:1907-12.

[32] Xu L, Yu G, Zhang E, Pan F, Yang K. In vivo corrosion behavior of Mg-Mn-Zn alloy for bone implant application. Journal of Biomedical Materials Research Part A 2007;83A:703-11.

[33] Agatonovic-Kustrin S, Beresford R. Basic concepts of artificial neural network (ANN) modeling and its application in pharmaceutical research. Journal of Pharmaceutical and Biomedical Analysis 2000;22:717-27.

[34] Almeida JS. Predictive non-linear modeling of complex data by artificial neural networks. Current Opinion in Biotechnology 2002;13:72-6.

[35] Liparini A, Carvalho S, Belchior Jadson C. Analysis of the applicability of artificial neural networks for studying blood plasma: determination of magnesium ion concentration as a case study. Clinical Chemical Laboratory Medicine2005. p. 939.

[36] Conway J, Liparini A, de Oliveira J, Belchior J. Analyses of the temperature and pH effects on the complexation of magnesium and calcium in human blood plasma: an approach using artificial neural networks. Analytical and Bioanalytical Chemistry 2007;389:1585-94.

[37] Smith JR, Knight D, Kohn J, Rasheed K, Weber N, Kholodovych V, et al. Using Surrogate Modeling in the Prediction of Fibrinogen Adsorption onto Polymer Surfaces. Journal of Chemical Information and Computer Sciences 2004;44:1088-97.

[38] Brauer DS, Rüssel C, Kraft J. Solubility of glasses in the system P2O5–CaO–MgO–Na2O–TiO2: Experimental and modeling using artificial neural networks. Journal of Non-Crystalline Solids 2007;353:263–70.

[39] Peng Q, Huang Y, Zhou L, Hort N, Kainer KU. Preparation and properties of high purity Mg–Y biomaterials. Biomaterials 2010;31:398-403.

[40] Haykin S. Neural Networks: A Comprehensive Foundation: Prentice Hall PTR; 1998.

[41] Riedmiller M, Braun H. A direct adaptive method for faster backpropagation learning: the RPROP algorithm Proceedings of 1993 IEEE International Conference on Neural Networks (ICNN '93) San Francisco, CA, USA1993. p. 586 - 91

[42] Huber N, Nix WD, Gao H. Identification of elastic-plastic material parameters from pyramidal indentation of thin films. Proceedings of the Royal Society of London Series A: Mathematical, Physical and Engineering Sciences 2002;458:1593-620.

[43] Neal RM. Bayesian Learning for Neural Networks. New York: Springer; 1996.

[44] Brar HS, Wong J, Manuel MV. Investigation of the mechanical and degradation properties of Mg–Sr and Mg–Zn–Sr alloys for use as potential biodegradable implant materials. Journal of the Mechanical Behavior of Biomedical Materials 2012;7:87-95.

[45] Sun Y, Zhang B, Wang Y, Geng L, Jiao X. Preparation and characterization of a new biomedical Mg–Zn–Ca alloy. Materials & Design 2012;34:58-64.

[46] Bornapour M, Muja N, Shum-Tim D, Cerruti M, Pekguleryuz M. Biocompatibility and biodegradability of Mg–Sr alloys: The formation of Sr-substituted hydroxyapatite. Acta Biomaterialia 2012.

[47] Kannan BM, Raman SRK. Evaluating the stress corrosion cracking susceptibility of Mg–Al–Zn alloy in modified-simulated body fluid for orthopaedic implant application. Scripta Materialia 2008;59:175-8.

[48] Kannan MB. Influence of microstructure on the in-vitro degradation behaviour of magnesium alloys. Materials Letters 2010;64:739-42.

[49] Gu X, Zheng Y, Cheng Y, Zhong S, Xi T. In vitro corrosion and biocompatibility of binary magnesium alloys. Biomaterials 2009;30:484-98.

[50] Xin Y, Chu PK. Influence of Tris in simulated body fluid on degradation behavior of pure magnesium. Materials Chemistry and Physics 2010;124:33-5.

[51] Xin Y, Hu T, Chu PK. Degradation behaviour of pure magnesium in simulated body fluids with different concentrations of. Corrosion Science 2011;53:1522-8.

[52] Xin Y, Huo K, Tao H, Tang G, Chu PK. Influence of aggressive ions on the degradation behavior of biomedical magnesium alloy in physiological environment. Acta Biomaterialia 2008;4:2008-15.

[53] Bohner M, Lemaitre J. Can bioactivity be tested in vitro with SBF solution? Biomaterials 2009;30:2175-9.

[54] Ellison G, Straumfjord JV, Hummel JP. Buffer Capacities of Human Blood and Plasma. Clinical Chemistry 1958;4:452-61.

[55] Li Y, Wen C, Mushahary D, Sravanthi R, Harishankar N, Pande G, et al. Mg–Zr–Sr alloys as biodegradable implant materials. Acta Biomaterialia 2012;8:3177-88.

[56] Zheng YF, Gu XN, Xi YL, Chai DL. In vitro degradation and cytotoxicity of Mg/Ca composites produced by powder metallurgy. Acta Biomaterialia 2010;6:1783-91.

[57] Kirkland NT, Birbilis N, Walker J, Woodfield T, Dias GJ, Staiger MP. In-vitro dissolution of magnesium–calcium binary alloys: Clarifying the unique role of calcium additions in bioresorbable magnesium implant alloys. Journal of Biomedical Materials Research Part B: Applied Biomaterials 2010;95B:91-100.

[58] Gu XN, Xie XH, Li N, Zheng YF, Qin L. In vitro and in vivo studies on a Mg–Sr binary alloy system developed as a new kind of biodegradable metal. Acta Biomaterialia 2012;8:2360-74.

[59] Liu CL, Wang YJ, Zeng RC, Zhang XM, Huang WJ, Chu PK. In vitro corrosion degradation behaviour of Mg–Ca alloy in the presence of albumin. Corrosion Science 2010;52:3341-7.

[60] Waizy H, Weizbauer A, Modrejewski C, Witte F, Windhagen H, Lucas A, et al. In vitro corrosion of ZEK100 plates in Hank's Balanced Salt Solution. BioMedical Engineering OnLine 2012;11:12.

[61] Merritt K, Brown SA, Sharkey NA. The binding of metal salts and corrosion products to cells and proteins in vitro. J Biomed Mater Res 1984;18:1005-15.

[62] Xin Y, Hu T, Chu PK. In vitro studies of biomedical magnesium alloys in a simulated physiological environment: A review. Acta Biomaterialia 2011;7:1452-9.

[63] Bergström CAS, Luthman K, Artursson P. Accuracy of calculated pH-dependent aqueous drug solubility. European Journal of Pharmaceutical Sciences 2004;22:387-98.

[64] Kiaer T, Grønlund J, Sørensen KH. Intraosseous pressure and partial pressures of oxygen and carbon dioxide in osteoarthritis. Semin Arthritis Rheum 1989;18:57-60.

[65] Zhang K, Zhu L, Fan M. Oxygen, a key factor regulating cell behaviour during neurogenesis and cerebral diseases. Frontiers in Molecular Neuroscience 2011;4.

[66] Valabregue R, Aubert A, Burger J, Bittoun J, Costalat R. Relation Between Cerebral Blood Flow and Metabolism Explained by a Model of Oxygen Exchange. J Cereb Blood Flow Metab 2003;23:536-45.

[67] Black CB, Huang HW, Cowan JA. Biological coordination chemistry of magnesium, sodium, and potassium ions. Protein and nucleotide binding sites. Coordination Chemistry Reviews 1994;135–136:165-202.

[68] Copeland BE, Sunderman FW. Studies in serum electrolytes: : XVIII The magnesium-binding property of the serum proteins. J Biol Chem 1952;197:331-41.

[69] Fogh-Andersen N. Albumin/calcium association at different pH, as determined by potentiometry. Clin Chem 1977;23:2122-6.

[70] Frye RM, Lees H, Rechnitz GA. Magnesium-albumin binding measurements using ion-selective membrane electrodes. Clinical Biochemistry 1974;7:258-70.

[71] Guillaume YC, Guinchard C, Berthelot A. Affinity chromatography study of magnesium and calcium binding to human serum albumin: pH and temperature variations. Talanta 2000;53:561-9.

[72] Guillaume YC, Peyrin E, Berthelot A. Chromatographic study of magnesium and calcium binding to immobilized human serum albumin. J Chromatogr B Biomed Sci Appl 1999;728:167-74.

[73] van Os GAJ, Koopman-van Eupen JHM. The interaction of sodium, potassium, calcium, and magnesium with human serum albumin, studied by means of conductivity measurements. Recueil des Travaux Chimiques des Pays-Bas 1957;76:390-400.

[74] Tie D, Feyerabend F, Hort N, Willumeit R, Hoeche D. XPS Studies of Magnesium Surfaces after Exposure to Dulbecco's Modified Eagle Medium, Hank's Buffered Salt Solution, and Simulated Body Fluid. Advanced Engineering Materials 2010;12:B699-B704.

[75] Cheng CP, Herfkens RJ, Taylor CA. Inferior vena caval hemodynamics quantified in vivo at rest and during cycling exercise using magnetic resonance imaging. American Journal of Physiology - Heart and Circulatory Physiology 2003;284:H1161-H7.

[76] Wexler L, Bergel DH, Gabe IT, Makin GS, Mills CJ. Velocity of Blood Flow in Normal Human Venae Cavae. Circulation Research 1968;23:349-59.

[77] Kane WJ. Fundamental Concepts in Bone-Blood Flow Studies. The Journal of Bone & Joint Surgery 1968;50:801-11.

[78] Witte F, Hort N, Vogt C, Cohen S, Kainer K, Willumeit R, et al. Degradable biomaterials based on magnesium corrosion. Curr Opin Solid State Mater Sci 2008;12:63 - 72.

Figure Captions

Fig. 1: Corrosion rate of cast Mg (measured by potentiodynamic polarisation) under varying experimental conditions (DMEM = cell culture medium, FBS = Fetal Bovine Serum) (unpublished data).

Fig. 2: Data base for the corrosion rate of extruded Mg under varying experimental conditions (buffer represented by NaCl concentration).

Fig. 3: Study of information content by providing a single parameter as an input; the increasing error is related to the decreasing importance of an input parameter.

Fig. 4: Study of information content by removing a single input; the decreasing error is related to the decreasing importance of an omitted input parameter; 'None' is the reference that includes all seven inputs (smallest error).

Fig. 5: Re-prediction of training patterns from five ANNs: a) Plot of predicted average versus measured corrosion rate; and b) Plot of the absolute error, sorted by value, versus normalised pattern number.

Fig. 6: Evaluation of the ANN prediction with respect to variation in NaCl and CO_2 under reference conditions (O_2 = 21%, T = 20°C, protein = 0%, $NaHCO_3$ = 0 mg/L); a) prediction of the expected value for the corrosion rate; b) standard deviation derived from five ANN predictions.

Fig. 7: Evaluation of the ANN prediction with respect to reference conditions by visualising the effect of individual parameters on the corrosion rate (decrease of O_2 from 21 to 5%, increase of temperature from 20 to 37°C, increase of protein from 0 to 20 vol%, and increase of $NaHCO_3$ from 0 to 3700 mg/L).

Figure(s)

Click here to download high resolution image

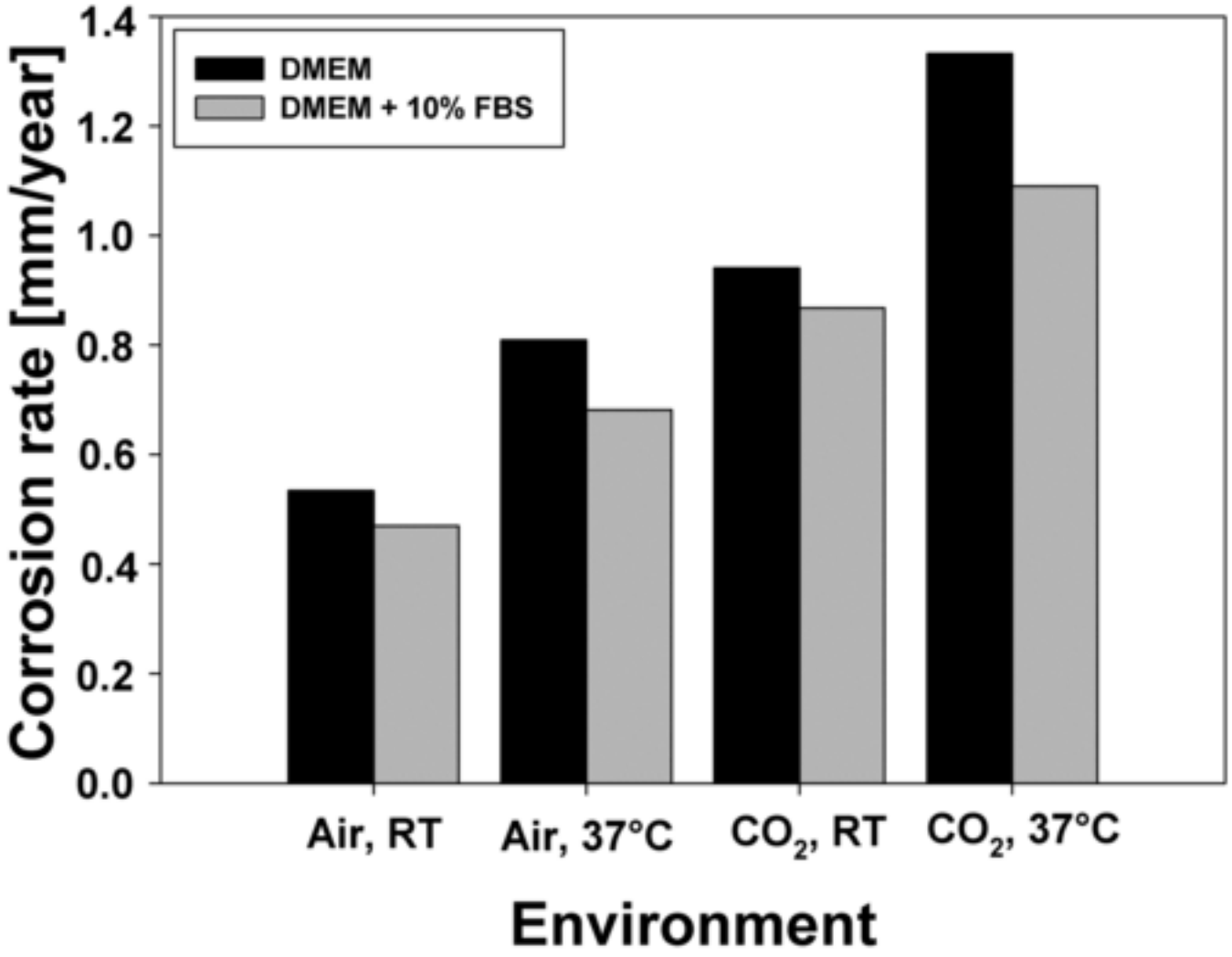

Figure(s)

Click here to download high resolution image

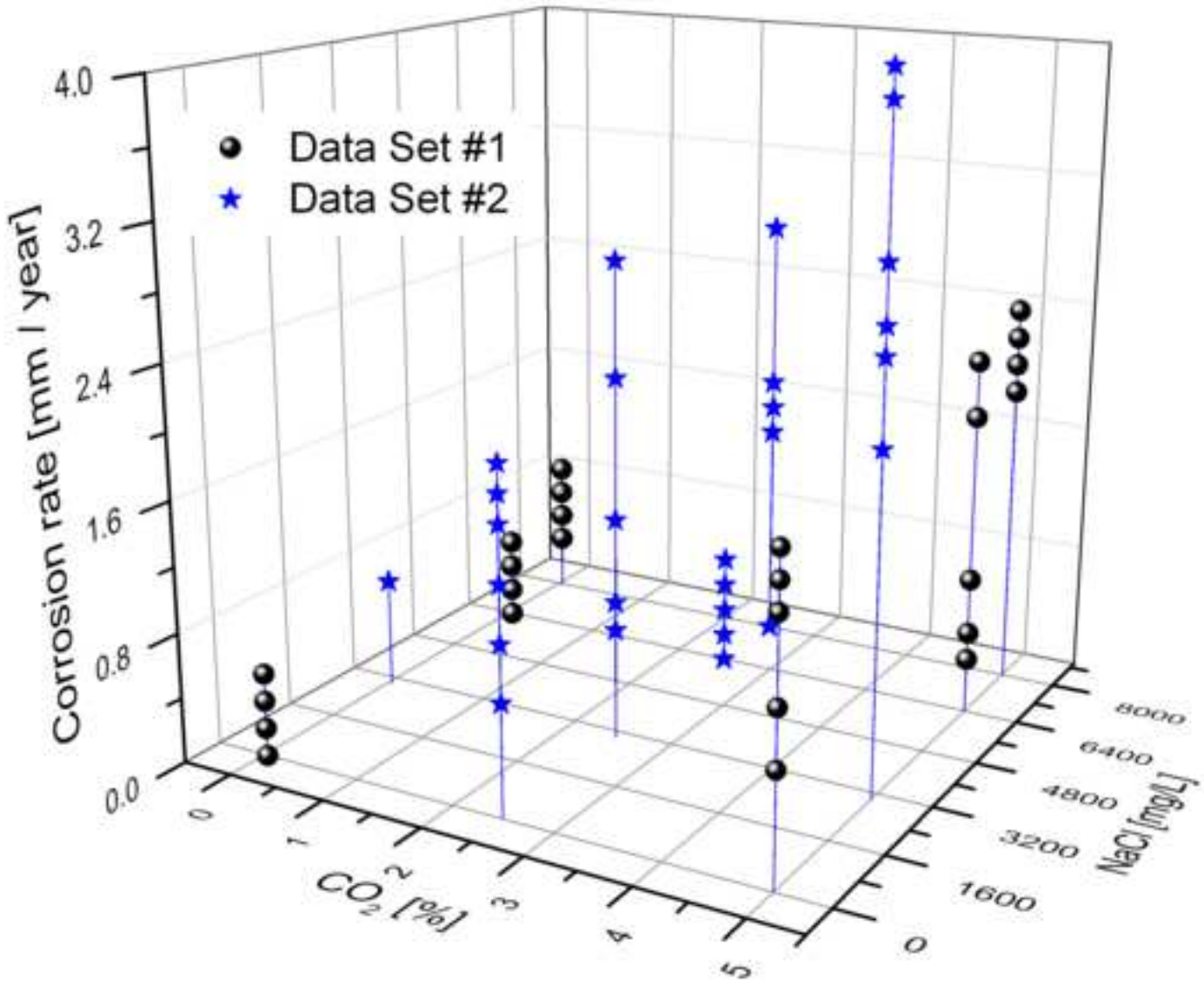

Figure(s)

Click here to download high resolution image

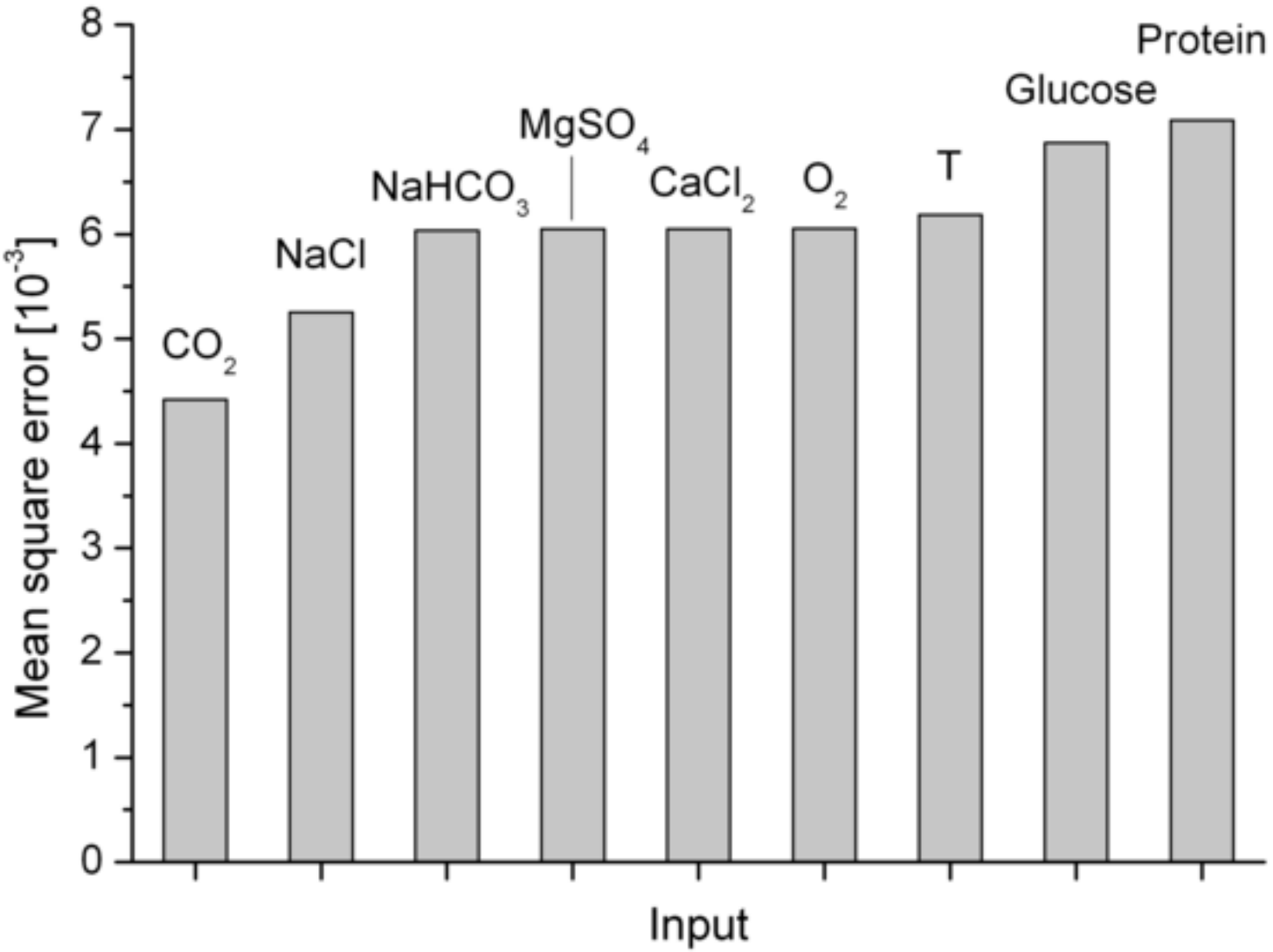

Figure(s)

Click here to download high resolution image

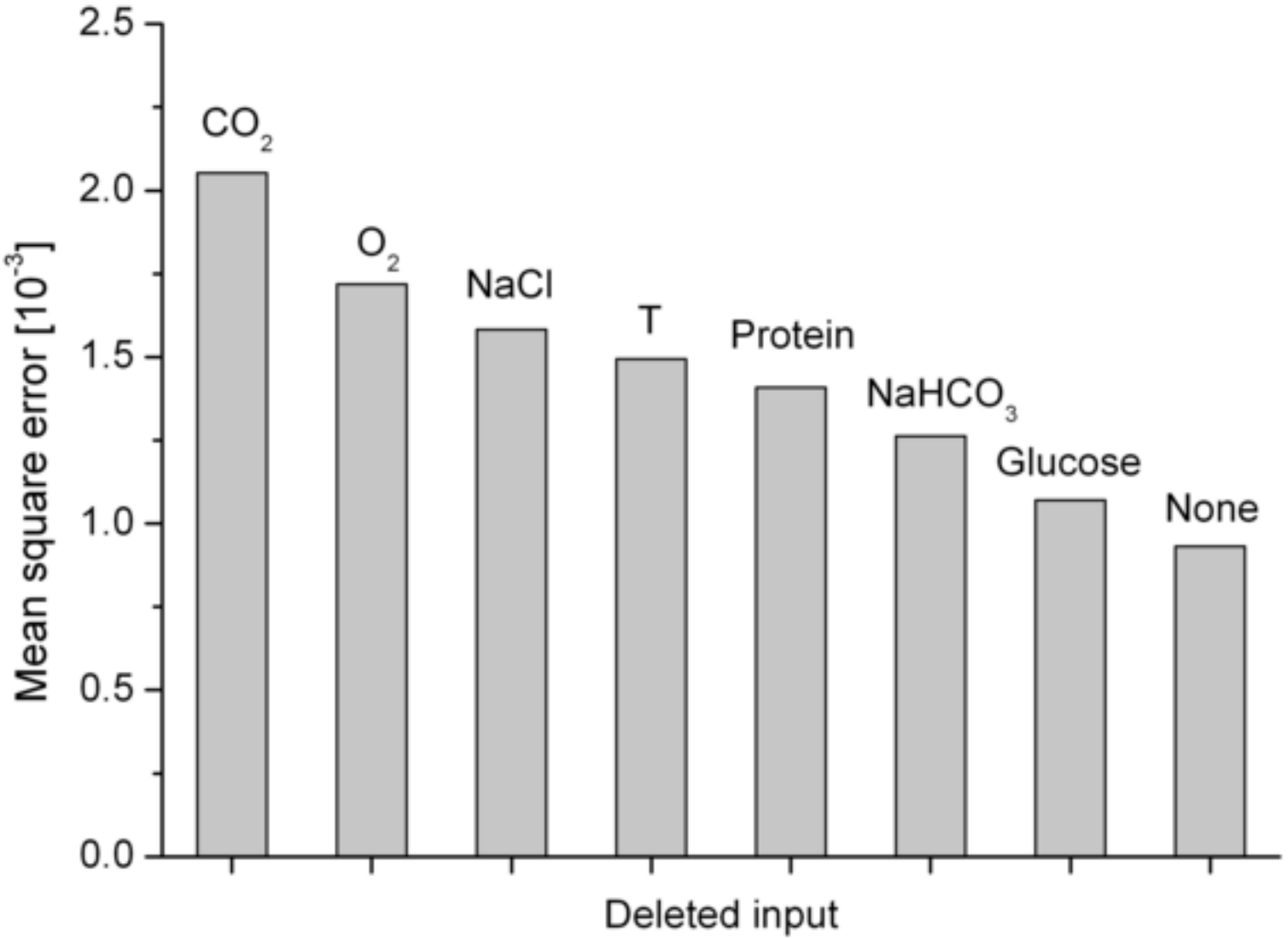

Figure(s)

Click here to download high resolution image

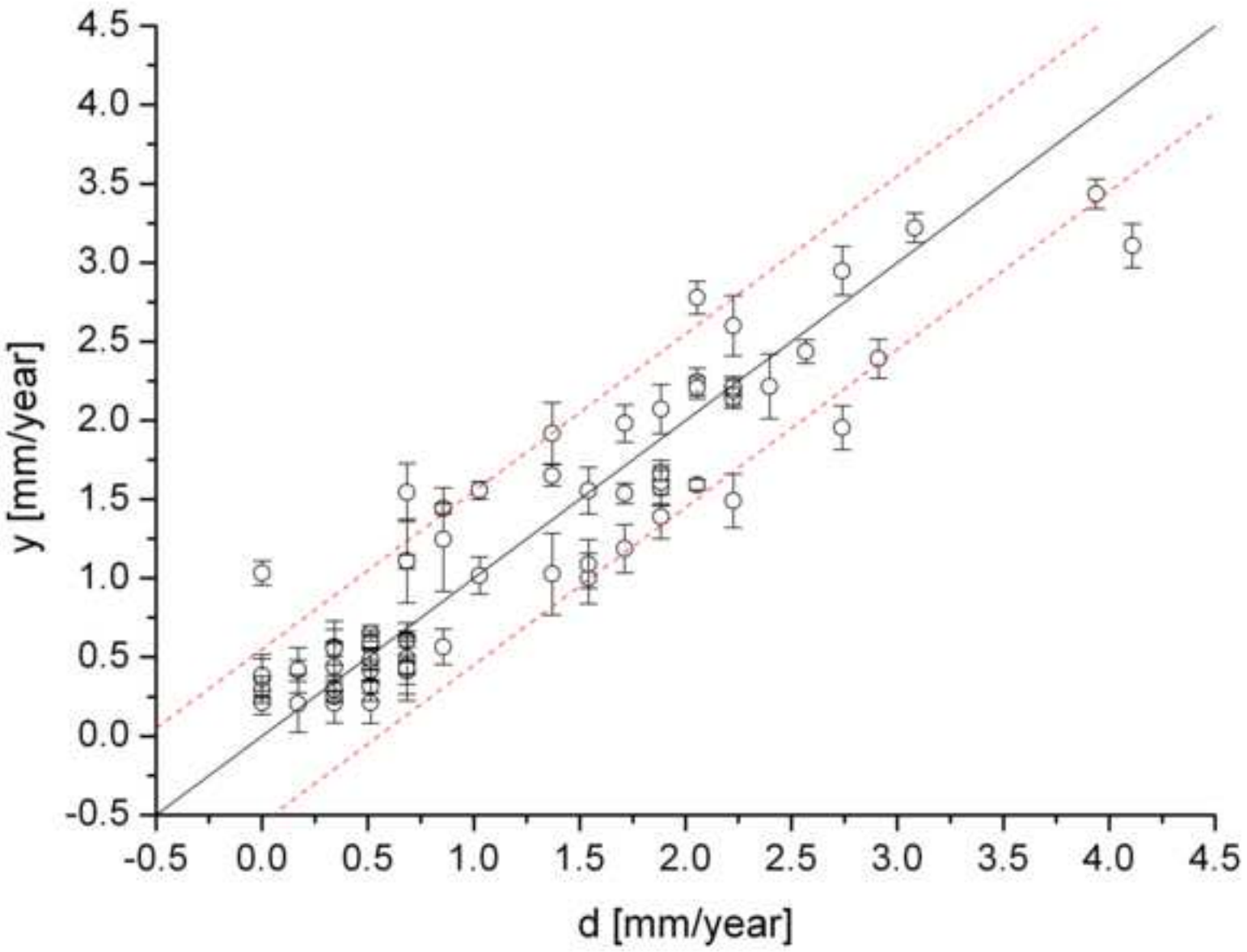

Figure(s)

Click here to download high resolution image

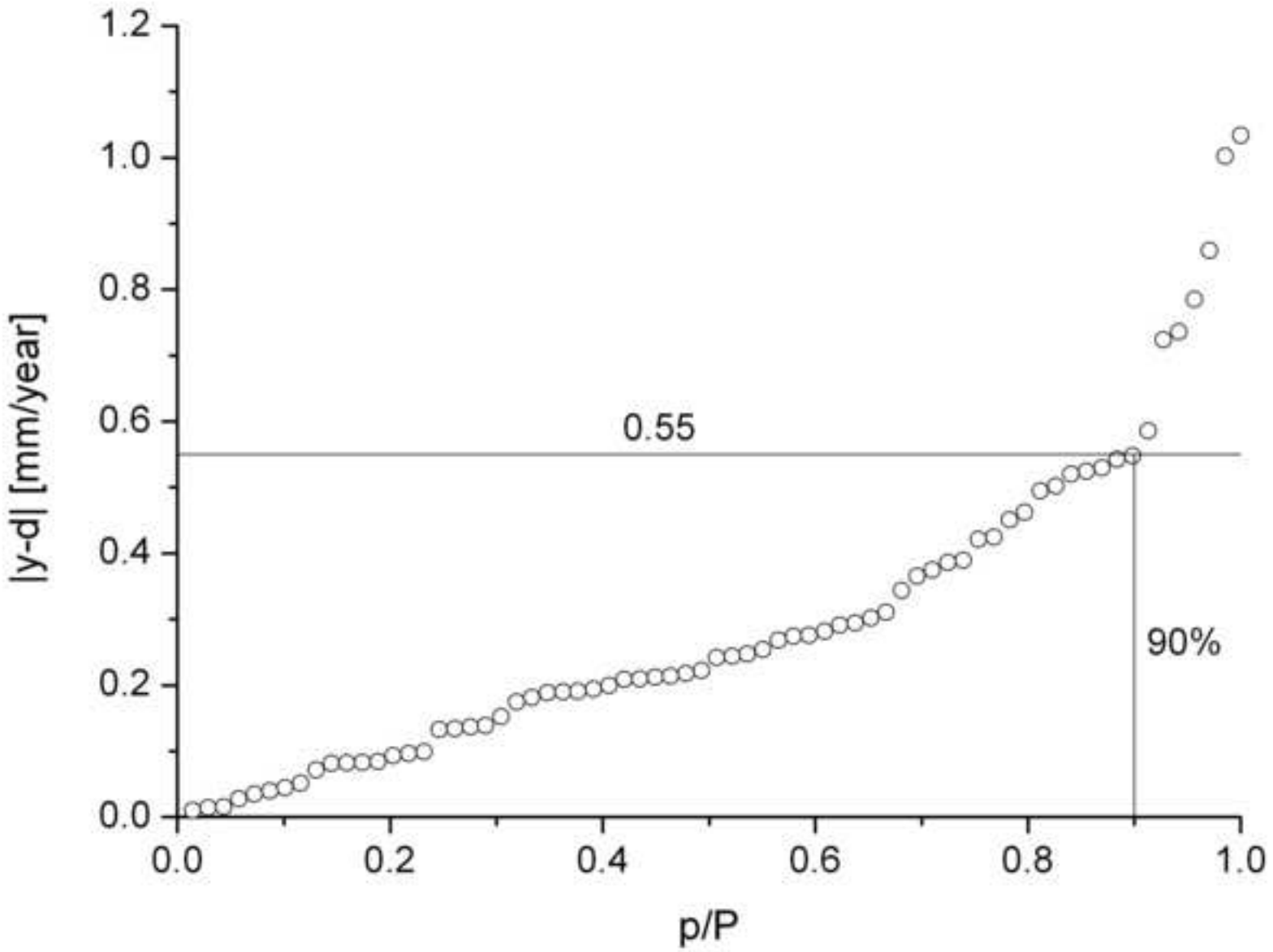

Figure(s)

Click here to download high resolution image

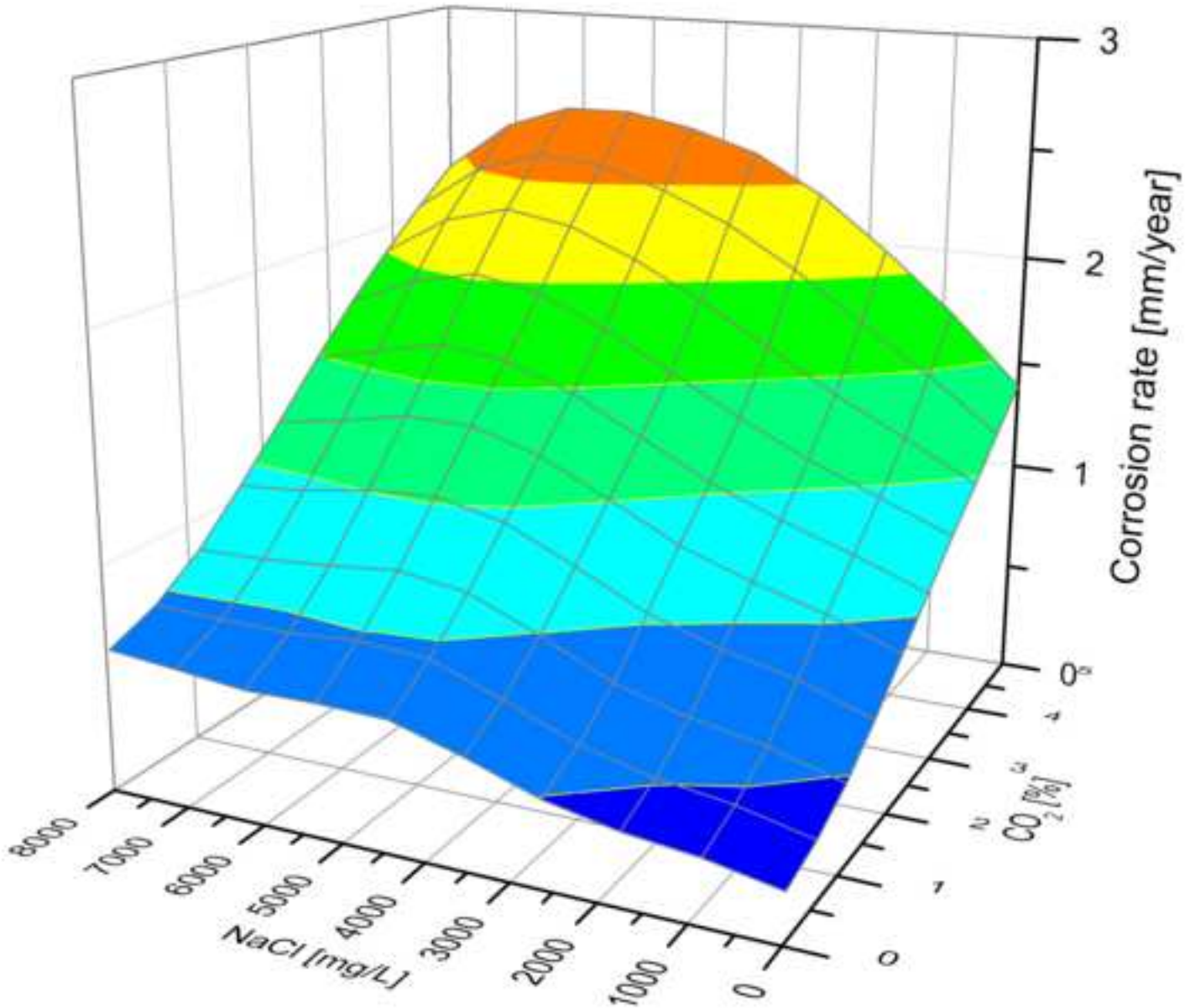

Figure(s)

Click here to download high resolution image

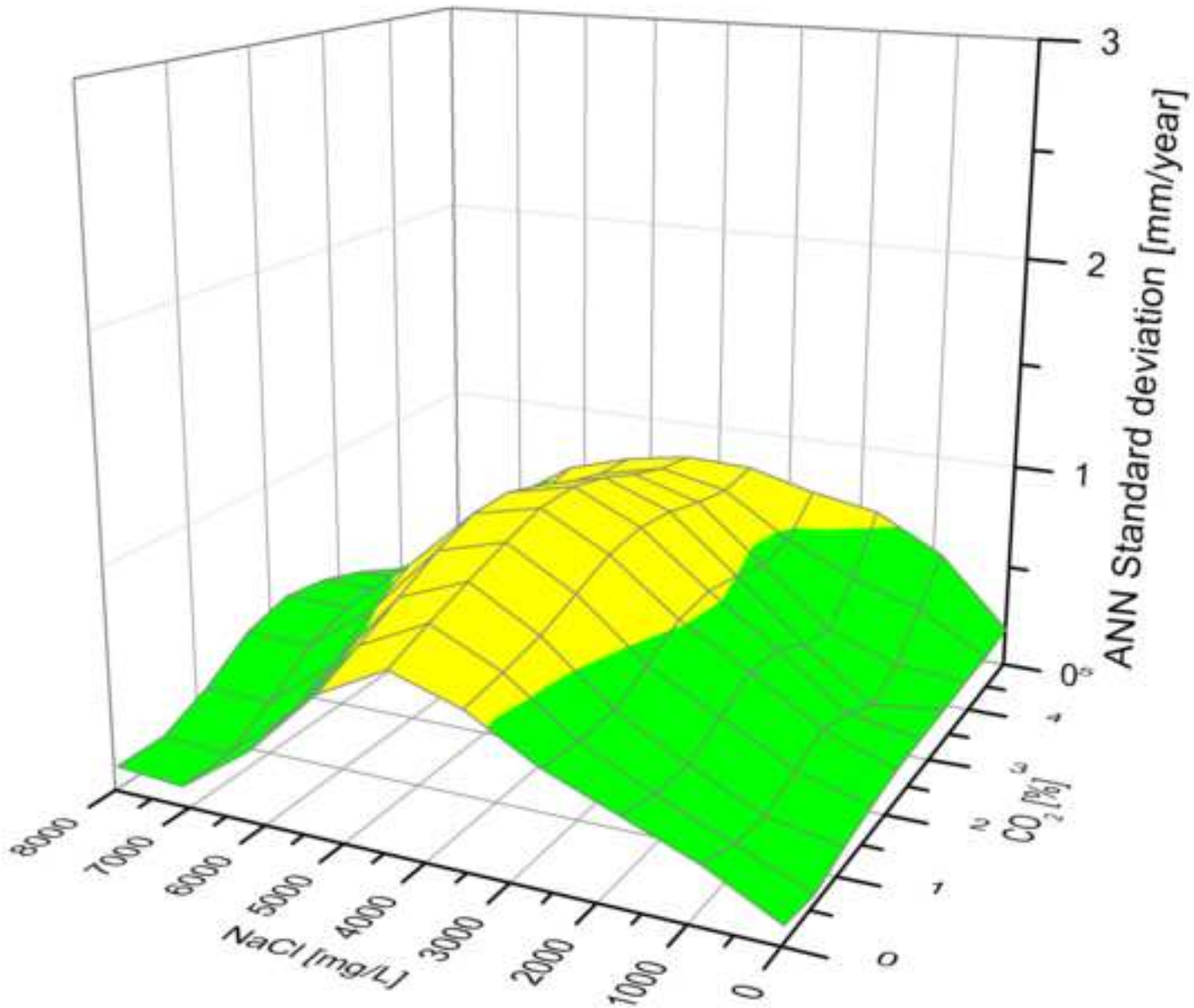

Figure(s)

Click here to download high resolution image

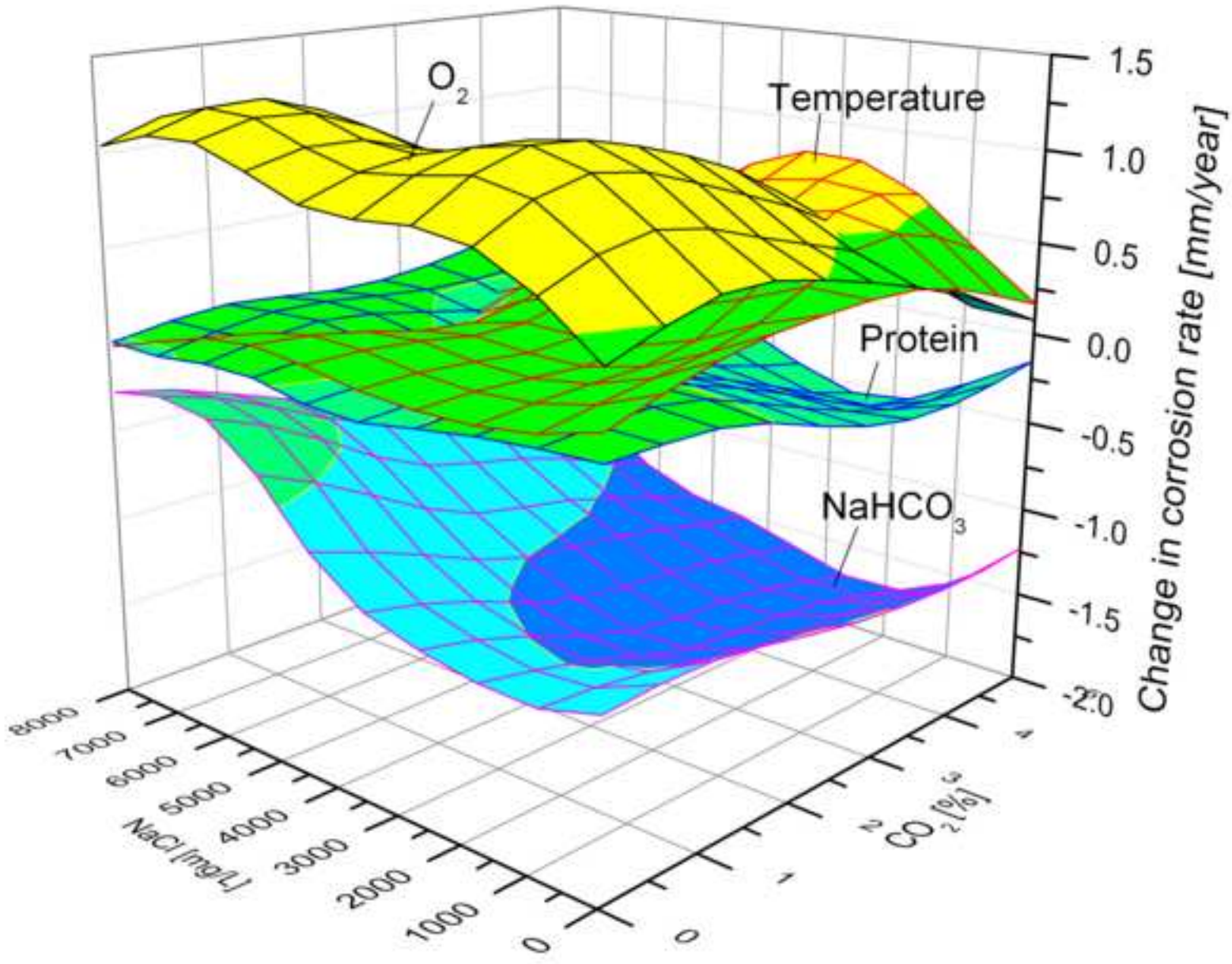

Tables

Table 1: Range of measured values and parameters; the compositions of different buffer systems are represented by the set NaCl, $NaHCO_3$, $CaCl_2$, $MgSO_4$, and glucose.

	Corrosion rate	**Protein (FBS)**	**Temperature**	**CO_2**	**O_2**
Unit	[mm/year]	[vol%]	[°C]	[%]	[%]
min	0	0	20	0.034	5
max	4.1	20	37	5.0	21

Buffer content	**NaCl**	**$NaHCO_3$**	**$CaCl_2$**	**$MgSO_4$**	**Glucose**
Unit	[mg/L]	[mg/L]	[mg/L]	[mg/L]	[mg/L]
min	0	0	0	0	0
max	8000	3700	264	200	4500

Table 2: Comparison of the partial pressure of oxygen and carbon dioxide in the atmosphere, blood and bone. The values were calculated based on [64]

	pO_2			**pCO_2**		
	Torr (mmHg)	kPa	%	Torr (mmHg)	kPa	%
Atmosphere (dry)	159.22	21.22	20.95	0.23	0.03	0.03
Arterial blood	111.2	14.82	14.63	31.3	4.17	4.12
Venous blood	36.3	4.84	4.78	40.5	5.39	5.32
Bone	34	4.53	4.47	50	6.65	6.56